Magnetic force microscopy study of electron-beam-patterned soft permalloy particles: Technique and magnetization behavior

Xiaobin Zhu and P. Grütter
*Center for the Physics of Materials, Department of Physics, McGill University, 3600 University Street,
Montréal, Québec, Canada H3A 2T8*

V. Metlushko
Department of Electrical and Computer Engineering, University of Illinois at Chicago, Chicago, Illinois 60607-0024

B. Ilic
School of Applied and Engineering Physics, Cornell University, Ithaca, New York 14853

Electron-beam-patterned submicron permalloy elements with different aspect ratios were studied by magnetic force microscopy (MFM). The MFM tip stray field can be used to control a particle's magnetic state. By suitably choosing the operating mode and tip coatings, the tip induced distortion of the magnetic structure of soft permalloy elements can be largely reduced. The particle switching field can be precisely obtained by operating MFM at remanence. Through studying the remanent magnetization behavior, it was revealed that for large aspect ratio elements ($>4:1$) magnetization reversal occurs directly from one single domain state to the reversed single domain state, while for medium aspect ratio elements ($\leq 4:1$) the magnetization reversal occurs in a two-step process with two characteristic switching fields. Initially single domain particles switch into a low moment state (vortex state) at the first field H_s, while at the higher field H_a, the magnetic moments form a reversed single domain state. The forming of the low moment state is due to the fact that the vortex states can be trapped in the elements during magnetization reversal. This is consistent with micromagnetic simulations and can be directly demonstrated by controlled local MFM tip induced switching. The variations in the measured distribution of the switching fields for both large and small aspect ratio particle arrays are attributed to different reversal mechanisms as well as individual difference in size, thickness, and edge roughness.

PACS number(s): 75.60.Jk, 68.37.Rt, 75.75.+a, 07.79.Pk

I. INTRODUCTION

Patterned magnetic elements are currently widely studied due to fundamental issues and their potential practical application in ultrahigh density storage and magnetoresistive random access memory.[1–8] Experimental investigation of small magnetic elements are crucial tests of micromagnetic codes and lead to a better understanding of their magnetization reversal behavior. Due to its high spatial resolution and high sensitivity, magnetic force microscopy (MFM) is an ideal tool to study the magnetic structures and magnetization reversal of submicron magnets.[9] Furthermore, by choosing large area scans, MFM can also be used to characterize the ensemble magnetization behavior within the presence of external magnetic fields.[10] However, it is challenging to obtain nondistorted images by MFM due to the mutual interaction of the MFM tip with a magnetic sample. The situation is at its worst when using large moment tips (leading to large signals) to study soft magnetic materials.[11] In the first part of this paper, we will discuss how to minimize the MFM tip's stray field induced irreversible distortion of the particle's magnetic state and present a method allowing the systematic determination of a particle's switching field from MFM images.

Recent studies show that the material, size, and shape of the particles have a strong influence on the particle magnetic state and reversal behavior.[1–8] For elongated rectangular particles, with small width, the shape anisotropy dominates and forces the magnetic moments to lie along the long axes of the elements. Relevant issues related to the reversal characteristics of such particles are the formation of binary states, the uniformity as well as the reproducibility of switching fields. As the element size is still much bigger than the exchange length of the magnetic material, trapping of domain walls and the formation of vortices can make the reversal behavior ill defined.[4,12] In the second part of this paper, we will study a series of arrays of particles with different aspect ratios. We study the switching mechanism and determine the switching field distributions. We found vortex formation not only appears in the reversal of small aspect ratio particles, but also for particles with an aspect ratio as large as 4:1 with width of 200 nm, and lead to a broad switching field distribution.

II. EXPERIMENTAL TECHNIQUES

A. Sample preparation

Elliptical permalloy submicron elements with different aspect ratios from 1:1 to 10:1, with widths of 100, 150, and 200 nm, and nominal thickness of 30 nm, were prepared by standard e-beam lithography, e-beam deposition, and liftoff techniques.[13] The hysteresis loop of unpatterned film shows the coercivity is less than 3 Oe. Figure 1 shows scanning electron microscopy (SEM) images of two typical arrays.
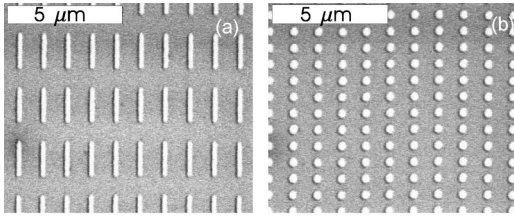
FIG. 1. SEM images of two typical permalloy arrays.

B. Magnetic characterization

MFM images were taken in tapping/lift mode,[14] constant frequency shift mode,[15] and constant height mode, with different magnetic tips. In tapping/lift mode, topography and magnetic contrast can be well separated. The sample topography is obtained in the tapping part of the scan, where the cantilever oscillation amplitude reduction is maintained constant by a feedback loop. Magnetic contrast is subsequently obtained in the lift mode by monitoring the cantilever's frequency or phase shift upon rescanning the previously measured topography with a user controlled height offset. In the constant frequency shift mode a feedback circuit adjusts the tip–sample separation in order to keep the cantilever resonant frequency constant. It is challenging to study magnetic nanoparticles in this mode, as a dc voltage is usually applied to the sample in order to stabilize the feedback.[9] For patterned arrays, the topography differences between substrate and particles can lead to a strong convolution of magnetism with topography. In the constant height mode, instead of tracking the sample surface, the tip scans across the surface at a predetermined height while the cantilever frequency shift is monitored. Unavoidable sample tilt is compensated by tilt correction hardware. By applying a suitable voltage between the tip and sample (typically less than 100 mV, although it varies depending on the tip sharpness and the material differences), the electrostatic force due to contact potential differences between tip and sample can be minimized. In this mode, we found that the interaction force is dominated by the magnetic contribution even for tip–sample separations as small as 20 nm.

The force sensors used for the MFM images presented in this paper are thin film coated nanosensor silicon cantilevers. The silicon cantilevers have a typical spring constant of 1 N/m, resonance frequency of 70 kHz, and quality factor of 150 in air and 40 000 at 1.0×10^{-5} Torr. The tips were sputter coated with films of NiCo, NiFe, and CoPtCr of varying thicknesses, and subsequently magnetized along their axis prior to imaging. To study the magnetization reversal, an in-plane *in situ* calibrated electromagnet was used[16] which can apply to fields up to 1000 Oe.

III. EXPERIMENTAL RESULTS AND DISCUSSION

A. Techniques

There is an unavoidable mutual interaction leading to potential distortions between an MFM tip and sample magnetization during imaging. It is therefore very crucial to characterize the tip stray field and its spatial distribution. Recently, the tip's stray field has been quantified by sophis-
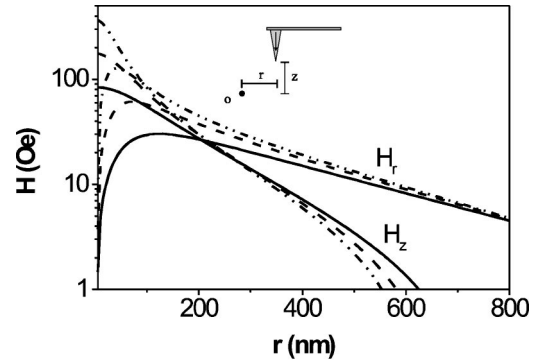
FIG. 2. Calculated tip stray field of a low moment tip as a function of lateral distance r and at different z, indicated in the inset; solid line: $z = 100$ nm, dashed line: $z = 50$ nm, dash dot dot line: $z = 20$ nm. Tip: 30 nm CoPtCr.

ticated techniques, such as micro-Hall sensors,[17] Lorentz electron tomography,[18] and electron holography.[19] The tip stray field can also be obtained by quantitative calibrated MFM.[20] It turns out that simple model calculations give a reasonable estimate of the tip stray fields.[9,21] In our model calculation, we assume the tip has conical geometry. The cone half angles of the silicon tip before and after coating are both 17°. The radius of the silicon tip r_0 is 10 nm, while the radius of the coated tip is assumed to be half of the total of the silicon tip radius and the coating thickness. The tip is magnetized along the z direction in a field of 1 T, and the tip moment is assumed to be aligned along the z axis. The saturation magnetization of the coating material is 450, 800, 1000 emu/cm^3 for CoPtCr, NiFe and NiCo, respectively. Figure 2 gives a typical example of the calculated stray field of a 30-nm CoPtCr coated tip at various tip–sample separations (z) and different lateral distances (r). As expected, the stray field close to the tip end is substantial (a few hundred oersted at distances of a few tens of nanometers). The calculated stray field and decay characteristics are consistent with the experimental data.[18] We would like to point out a less appreciated fact: the radial component is also substantial and decays much slower than that of the z component. At lateral distances of a few hundred nanometers, the radial component can thus be larger than the z component.[21] In Table I, a list of MFM tips used in our experiments as well as characteristic field strengths and widths are presented.

Magnetic tips can lead to substantial distortion of soft magnetic samples. The distortion includes local magnetization of the sample,[22] reversible domain wall displacement,[23]

TABLE I. A list of tip's stray field and field distribution for some tips used in the experiment at $z = 20$ nm.

Tip coating	CoPtCr	CoPtCr	CoPtCr	NiFe
Thickness (nm)	15	30	50	60
z stray field (Oe)	280	360	460	900
z half width at half maximum (nm)	60	100	130	150
r stray field (Oe)	60	120	160	320
r width (nm)	240	280	400	420
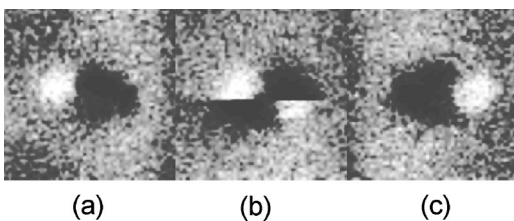
FIG. 3. (a)–(c) Three consecutive scans of the same 500 nm $\times$ 200 nm particle; The tip is a 60-nm permalloy coated probe, and the images are acquired in air using the tapping/lift mode with a lift height of 80 nm on a DI Multimode Nanoscope.

and irreversible domain wall displacement.[24] Despite these issues, MFM has still been successfully used to study soft magnetic domain structures, such as those in iron whiskers or garnets by choosing proper magnetic tips.[25,26] This is due to the fact that the tip stray field is very local, and it cannot globally change the domain pattern. Minimization of the total magnetic energy of the sample will restore the domain wall to its original position. This is in contrast to the situation when studying nanoparticles, where the local tip stray field can extend over the entire particle volume. If the particle has a low switching field, tip induced magnetization reversal can easily occur. This effect is extremely serious when the MFM is operated in tapping/lift mode, due to the fact that the tip is extremely close to the particle while acquiring topography data. A typical tip induced magnetization reversal is shown in Fig. 3. Figures 3(a)–3(c) show three consecutive scans along a particle long axis. The first image showing bipolar contrasts indicates that the nanoparticle is in a single domain state. The second scan shows that the particle has a double domain like structure. Close inspection of the data shows that the contrast changed during a single scan line, indicating that the tip stray field reversed the particle's moment. The third image shows the same particle forming a single domain state, but with reversed orientation compared with the first image. These kinds of reversal are very common in large area scans, and multiple reversal of the same particle can be observed.

To minimize the tip stray field induced magnetic distortion, we found that the experiment needs to be performed in constant height mode with a low moment tip. In constant height mode, the tip–sample separation is controllable. Using a large tip–sample separation, one can greatly limit and control the tip stray field induced distortion. As an example, Fig. 4 shows a MFM image at constant height mode of an array of particles with dimensions of 600 nm $\times$ 150 nm. With this low moment tip no visible distortion could be detected even at tip–sample separation as close as 20 nm. The reduced measurable signal of low moment tips can be compensated by operating the MFM in (moderate) vacuum,[15] allowing fine magnetic details of the elements to be observed even though the particle width is only 150 nm. Operation in constant height mode does not exclude tip stray field induced particle moment reversal. In fact, previous studies show that by reducing the tip–sample separation at a selected location above the particle the tip stray field can induce controlled and reproducible moment reversal.[11] We would like to point out that it is easy to detect tip stray field induced magnetiza-
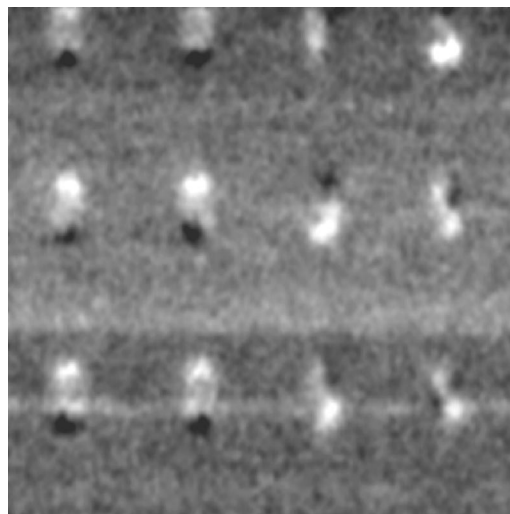
FIG. 4. MFM images of particle array with particle size of 600 nm $\times$ 150 nm. Tip: 15-nm CoPtCr; Tip–sample separation: 30 nm; in vacuum.

tion reversal in the constant height mode, which shows up as a discontinuity in the scan line. This is in contrast to the tapping/lift operation mode, where in many cases only a change in the scan angle provides indications of irreversible tip–sample interaction effects.[11] Note that in tapping/lift mode the low moment tip can still apply a substantial magnetic field to the particle while acquiring topography. A second benefit of constant height imaging is the potential increase in signal to noise (no extra noise contribution by the feedback control) and the increased possible scan speeds. Finally, the observed contrast in constant height mode allows a straightforward comparison with simulation, since each image consists of the force gradient at a fixed tip–sample separation. However, the disadvantage of this operating mode we found is that it requires the sample to be quite flat, the minimal tip–sample separation is determined by the sample roughness. However, if necessary, the topography can directly be tracked by noncontact methods using modulated electrostatic interactions.[27] For the present study this option was not implemented.

By doing MFM with an external magnetic field,[10,28] the nanoparticle magnetization behavior and switching field can be characterized and quantified. One needs to be aware of the fact that for submicron magnets, the combined effects of the MFM tip's stray field and the external magnetic field can make the particle switch at a lower field during imaging, as shown in Fig. 5. Figure 5(a) shows that all the particles form single domain states with the same moment orientation after saturation, while Fig. 5(b) shows MFM images acquired with a magnetic field of 60 Oe along the particle long axis. Some particles were directly switched to the reversed state by the external field, however, several others switched during the imaging process, resulting in the same contrast (dark) at both ends. Similar phenomena have been observed by some other research groups.[6,10,29,30] In this case the particle switching field is the combination of the external field and tip stray
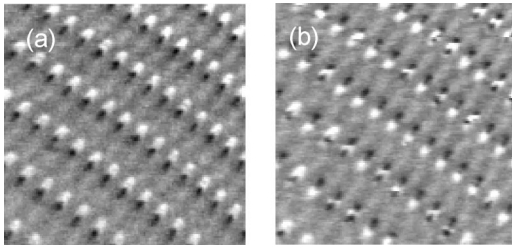
FIG. 5. MFM images of particle array with particle size of 1.2 μm$\times$200 nm. (a) remanet state after saturation;(b) in the presence of external field of 60 Oe along long axis. tip: 50-nm CoPtCr, tip–sample separation: 80 nm; in vacuum.

field. Since the tip stray field is omnidirectional and not homogeneous (Fig. 2), the real switching field of the particle cannot be easily obtained.

To minimize these effects and obtain accurate switching fields for the submicron particles, the experiment is performed at remanence after the field is ramped to a fixed value. In this case, reversible magnetization behavior of the elements cannot be revealed, but the irreversible magnetization behavior, such as switching, can be clearly observed. This method is especially suitable for studying single domain particles. By studying arrays of submicron magnetic particles, the remanent ''magnetization curve'' of the ensemble as well as individual particles can be obtained. This can be directly compared to remanent magnetization behavior characterized by other techniques, such as alternating gradient magnetometery(AGM).[31] As an example, Fig. 6 shows the different moment states after applying external fields to elliptical particles with an aspect ratio of 6:1 and a width of 200 nm. The particles can hold their single domain state until the external field reaches a critical value H_s, at which point the particle moments are suddenly reversed to the opposite single domain state. H_s is therefore the switching field of the elements.
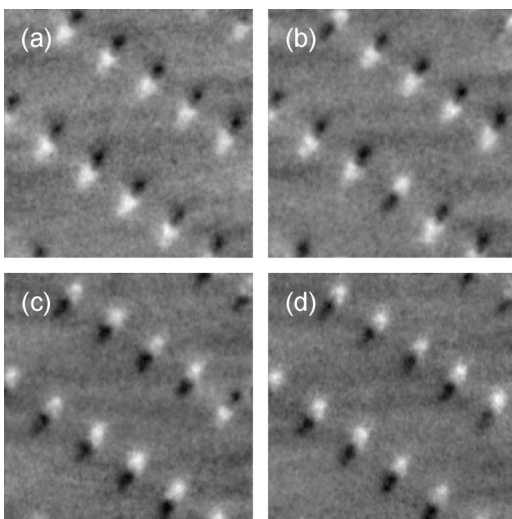
FIG. 6. Magnetization reversal as a function of external magnetic field. Imaged in the remanent states after the field ramped along particle long axis. (a) -200 Oe; (b) 75 Oe; (c) 90 Oe; (d) 101 Oe. Particle size: 1.2 μm$\times$200 nm, tip: 50-nm CoPtCr, lift height 120 nm.
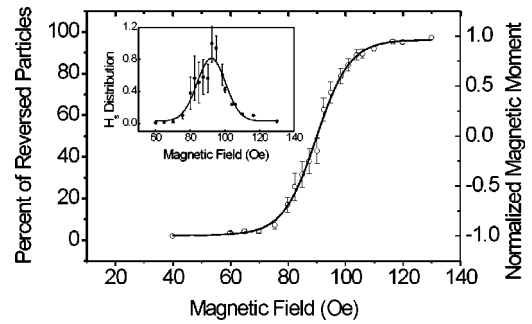
FIG. 7. (a) Percentage of reversal as function of field. Particle aspect ratio 7:1, width 200 nm; inset: switching field histogram.

The particle switching field value can be obtained very precisely if care is taken to ensure that the tip's stray field itself does not reverse the particle's moment. The achievable accuracy is determined by the minimal field ramping step, typically 1 Oe in this study. By using a small moment tip, operating at constant height, and measuring at remanence, we found the switching field even lower than 50 Oe can still be obtained reproducibly.

B. Magnetization reversal

In the following, we use constant height mode imaging of the remanent magnetization to observe reproducible and well-defined particle magnetic structures and systematically characterize their magnetization reversal. Figure 7 shows the percentage of reversed particle as a function of external magnetic field for a particle with aspect ratio of 7:1 and width of 200 nm. The results are averaged over 600 individual particles through 10 different images at different location. Each image contains about 60 individual particles, and the error bar is the statistical deviation of the 10 different images.

The switching mechanism is aspect ratio dependent. We found that for particles with aspect ratios less than 2:1 and width of 200 nm, the remanent state of the particle cannot hold single domain state, by showing low contrast at remanence. This is due to increased demagnetization field along the long axis as the aspect ratio decreases. The typical hysteresis curve for this kind of array looks like Fig. 1(b) of Ref. 32, with a negative switching field. Through our MFM investigations, we found that for particles with aspect ratios larger than 4:1 and widths of 200 nm, the switching takes place via a sudden moment reversal from one single moment state to the reversed single domain state, as shown in Fig. 6. Elliptical particles with large aspect ratios are generally believed to form single domain states without trapping end domains at both ends of the element.[33] However, we observed a small percentage (2%) of particles which formed a low moment state at remanence after switching. This percentage increases as the particle aspect ratio decreases, as shown in Fig. 8. The low moment states are circled as a guide to the eyes.

To further clarify the magnetization behavior and elucidate the nature of the low moment state, we plot remanent magnetization curves[34] of three typical particles, as shown in Fig. 9. A very small percentage of the particles appear to
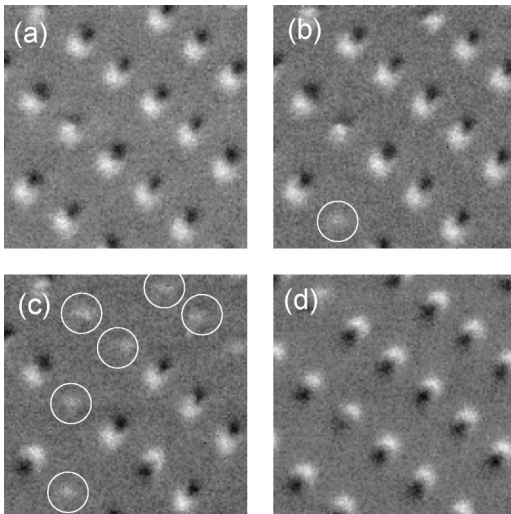
FIG. 8. Reversal as a function of external magnetic field after saturation at -250 Oe, (a) 50 Oe, (b) 70 Oe, (c) 90 Oe, (d) 180 Oe. Particle size: 800 nm×200 nm; circled: low moment states.

reverse directly [Fig. 9(a)], similar to the typical behavior of particles with large aspect ratios. However, most particles behave as shown in Fig. 9(b). A broad flat region with low moment state of about 50–100 Oe width is found. This observation is similar to measurements by AGM of the remanent magnetization curve of low aspect ratio permalloy arrays with size $1.2 \mu m \times 0.9 \mu m$.[31]

The patterned particles do not have uniform switching behavior. The average switching field and switching field
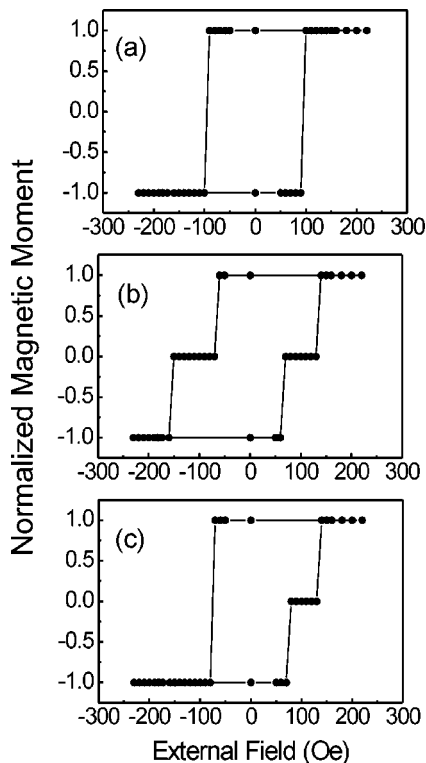
FIG. 9. Remanent hysteresis of three different individual particles in Fig. 8.
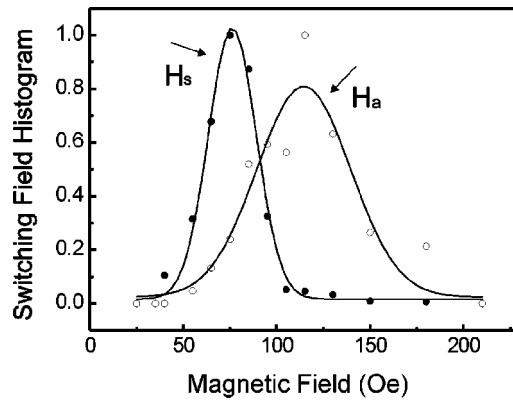
FIG. 10. Switching field histogram of the particle array with particle size of 800 nm×200 nm.

distribution can be obtained through the magnetization derivative curve, dM/dH, which is sensitive to the total magnetic moment.[35] MFM allows the determination of the average switching field as well as the switching field distribution of ensembles and of individual particles. A typical example of a switching histogram is shown in the inset of Fig. 7 with array of aspect ratio of 7:1. The peak shows that the ensemble of particles has an average switching field of 90 Oe. However, there are a few percent switched at fields below 70 Oe and a few percent above 110 Oe. By fitting the curve with a Gaussian distribution, we found that the full width of the peak is about 32 Oe, 36% of the average switching field. The switching field distribution arises from differences in the individual particle switching fields. The particles contributing to the extreme tails of the distribution can be readily identified.

We used two fields to characterize the switching behavior of medium aspect ratio particles (4:1): H_s, at which the particle switches directly from the single domain to a low moment state and H_a at which a reversed single domain is formed from the low moment state. Figure 10 plots the histogram of these two fields. As we can see, two peaks appear, with $\langle H_s \rangle$ much smaller than $\langle H_a \rangle$. δH_s has comparable width to that of large aspect ratio particles, while δH_a is much broader.

We found that as the aspect ratio increases, the switching field H_s increases, consistent with the Stoner–Wohlfarth model.[36] However, the switching mechanism is not coherent rotation. Since the particle is much bigger than the exchange length, the switching occurs through nucleation. The natural switching field distribution of each individual particle is found to be very narrow due to its big size, and the distribution is in the limit of the field ramping step of our experiments (typically 1 Oe). The variations of switching field values are a consequence of the variation of the demagnetization fields as a result of observable differences in local defects, edge smoothness, and thickness. Even if one could directly observe the chemical homogeneity or variations in stress of individual elements, it is beyond our current modeling capabilities to determine how these variations effect the sample demagnetization field.

However, the switching field distribution can be broadened if different reversal mechanisms are involved, such as
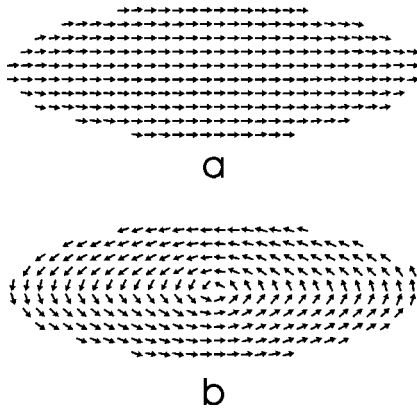
FIG. 11. Two different state in an elliptical particle. (a) single domain; (b) one vortex. Particle size 600 nm$\times$200 nm$\times$30 nm; unit size: 10^3 nm^3.

FIG. 12. Local tip stray field induced magnetization reversal. Tip located at different position above the particle can lead to different magnetic states: (a), (b), and (c). Tip: 50-nm CoPtCr, constant height mode in vacuum, particle size 600 nm$\times$150 nm.

trapping a vortex during a reversal process.[12,31] Since the particle size is still much bigger than the exchange length of permalloy materials, even for a medium aspect ratio array (4:1), the vortex can still be formed in the dynamic reversal process, and can be energetically stable in the remanent state, which eventually makes the switching not reproducible and broadens the switching field distribution. Micromagnetic simulations suggest that both the single domain state and the vortex state could be formed in the same elliptical particle. Figure 11 shows an example of an elliptical particle with size 600 nm$\times$200 nm$\times$30 nm. The simulations were performed using the publicly available newly released three-dimensional micromagnetic code from NIST.[37] The unit size for the simulation is 10 nm$\times$10 nm$\times$10 nm. We found that the total energy of the two states is very close, with the vortex state being only 5% higher than the single domain state. For the single domain state, the exchange energy is lower, but it has a higher demagnetization energy. Simulations from other groups also show that even multivortex states can be formed in elliptical permalloy particles.[38]

The trapping of a low moment state in an elliptical particle can directly be induced by using the stray field of the MFM tip. By positioning the tip at reduced tip–sample separations at different locations above a particle, different final magnetic states can reproducibly be obtained (see Fig. 12). When the tip is located at either end of the particle at small separation, the particle moment is switched back and forth due to the tip field associated switching. This can be verified by subsequent imaging at increased tip–sample separations [Figs. 12(a), (c)]. However, if we put the tip close to the center region of the particle (b), the particle forms a low moment state, either a multidomain or a vortex state. The formation of this low moment state is a direct consequence of the axial symmetry of the tip stray field, and as such the particle moment has no preference to switch in either of the two possible single domain states that are energetically only slightly lower.

During the switching process, if there is no vortex trapped in the particle, the switching will occur by directly switching to the reversed single domain state, as indicted in Fig. 9(a). However, if there is a vortex trapped in the element, a much
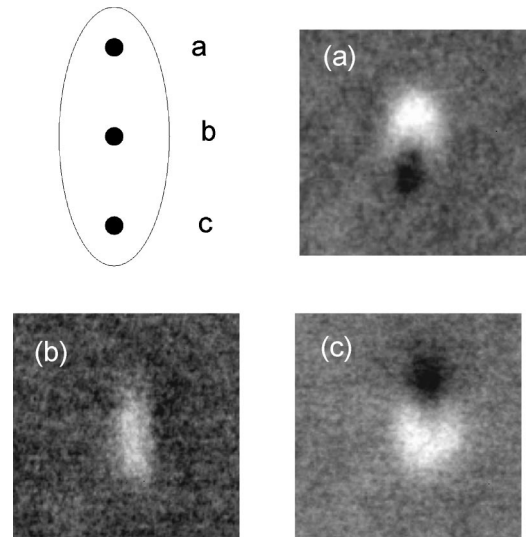
larger field H_a, is needed to expel the vortex out from the element in order to form a reversed single domain state. A field smaller than H_a can only make the vortex move reversibly, and leads to the same state at remanence, as shown in the flat low moment region in Fig. 9(b). We note that the reversal paths shown in Figs. 9(a) and 9(b) are statistical and not identical every time for a given particle. The poor reproducibility can be shown in Fig. 9(c), for this individual particle, the moment can be switched directly from the single domain state to the reversed single domain state, or switch via the formation of a vortex state.

In conclusion, we have shown that the MFM tip stray field can easily distort soft submicron magnetic particles, especially during imaging in the tapping/lift mode of operation. We found that these MFM tip influences of the sample magnetic structure can be considerably reduced by using tips with small magnetic moments and by operating the microscope in the constant height mode. Vacuum operation is then necessary to increase the signal to noise level. Magnetic particle switching fields can be precisely characterized by performing MFM at remanence after ramping the external field to a predetermined value. The magnetization reversal behavior is aspect ratio dependent. The switching field for different individual particles in the same array differs from each other, producing a broad distribution. For large aspect ratio (larger than 4:1), the switching proceeds directly from one single domain state to the opposite one with a fairly narrow switching field distribution. However for reduced aspect ratio particles, (even as high as 4:1), the particles first nucleate to a low moment stable or vortex state at smaller fields, and only switch to the reversed single domain state at higher fields. Depending on the aspect ratio of the particle, the vortex state and the single domain state are energetically very close. The resulting broad switching field distribution can be undesirable factors in the exploitation of such particles for practical uses.

[1] J.F. Smyth, S. Schultz, D. Kern, H. Schmid, and D. Yee, J. Appl. Phys. **63**, 4237 (1988); J.F. Smyth, S. Schultz, D.R. Frekin, D.P. Kern, S.A. Rishton, H. Schmid, M. Cali, and T.R. Koehler, *ibid.* **69**, 5262 (1991).

[2] G.A. Gibson and S. Schultz, J. Appl. Phys. **73**, 6961 (1993).

[3] M. Hehn, K. Ounadjela, J.-P. Bucher, F. Rousseaux, D. Decanini, B. Bertenlian, and C. Chappet, Science **272**, 1782 (1996).

[4] Jing Shi, S. Tehrani, T. Zhu, Y.F. Zheng, and J.-G. Zhu, Appl. Phys. Lett. **74**, 2525 (1999).

[5] R.E. Dunin-Borkowski, M.R. McCartney, B. Karynal, D.J. Smith, and M.R. Scheinfein, Appl. Phys. Lett. **75**, 2641 (1999).

[6] A. Fernandez and C.J. Cerjan, J. Appl. Phys. **87**, 1395 (2000); A. Fernandez, M.R. Gibbons, M.A. Wall, and C.J. Cerjan, J. Magn. Magn. Mater. **190**, 71 (1998).

[7] R.P. Cowburn, D.K. Koltsov, A.O. Adeyeye, M.E. Welland, and D.M. Tricker, Phys. Rev. Lett. **83**, 1042 (1999); R.P. Cowburn and M.E. Welland, Nature (London) **287**, 1466 (2000).

[8] J.-G. Zhu, Y. Zheng, and G.A. Prinz, J. Appl. Phys. **87**, 6668 (2000).

[9] P. Grütter, H. J. Mamin, and D. Rugar, *Scanning Tunnelling Microscopy II* (Springer, Berlin, 1992), pp. 151–207, and references therein.

[10] R.D. Gomez, M.C. Shih, R.M.H. New, R.F.W. Pease, and R.L. White, J. Appl. Phys. **80**, 342 (1996); R.D. Gomez, E.R. Burke, and I.D. Mayergoyz, *ibid.* **79**, 6441 (1996).

[11] X. Zhu, P. Grütter, V. Metlushko, and B. Ilic, J. Appl. Phys. **91**, 7340 (2002).

[12] Y. Zheng and J.-G. Zhu, J. Appl. Phys. **81**, 5471 (1997).

[13] P. Vavassori, O. Donzelli, V. Metlushko, M. Grimsditch, B. Ilic, P. Neuzil, and R. Kumar, J. Appl. Phys. **88**, 999 (2000).

[14] Digital Instruments, Santa Barbara, CA.

[15] T.R. Albrecht, P. Grütter, D. Horne, and D. Rugar, J. Appl. Phys. **69**, 668 (1991).

[16] The electromagnet is composed of soft iron bar with diameter of 1/2 in, with air gap of 1/2 in, the end of the bar is tapped with 45°. There are 4 000 turns of insulated copper wires wound on each bar. The center of the air gap can achieve 1000 Oe while applying 250-mA current. The field in the scanned area, typically less than 100 μm is very homogeneous. The field is measured with a Hall probe, which is calibrated with a calibrated Gaussmeter. The electromagnet produces negligible heat while applying 50-mA current to the electromagnets, however it will have heat considerably when applying 250-mA while operating in vacuum, which can induce the cantilever drift.

[17] A. Thiaville, L. Belliard, D. Majer, E. Zeldov, and J. Miltat, J. Appl. Phys. **82**, 3182 (1997).

[18] S. McVitie, R.P. Ferrier, J. Scott, G.S. White, and A. Gallagher, J. Appl. Phys. **89**, 3656 (2001).

[19] D.G. Streblechenko, M.R. Scheinfein, M. Mankos, and K. Babcock, IEE Tran. Magn. **32**, 4124 (1996).

[20] P.J.A. van Schendel, H.J. Hug, B. Stiefel, S. Martin, and H.-J. Güntherodt, J. Appl. Phys. **88**, 435 (2000).

[21] J.M. Garcia, A. Thiaville, J. Miltat, K.J. Kirk, J.N. Chapman, and F. Alouges, Appl. Phys. Lett. **79**, 656 (2001).

[22] A. Hubert and R. Schäfer, *Magnetic Domains, The Analysis of Magnetic Microstructures* (Springer, Berlin, 1998).

[23] Y. Liu and P. Grütter, J. Appl. Phys. **83**, 7333 (1998).

[24] U. Hartmann, Annu. Rev. Mater. Sci. **29**, 53 (1999).

[25] T. Göddenhenrich, U. Hartmann, M. Anders, and C. Heiden, J. Microsc. **152**, 527 (1988).

[26] Laurent Belliard, Ph.D. thesis, Universite de Paris-Sud Center D'Orsay, 1997.

[27] C. Schönenberger and S.F. Alvarado, Z. Phys. B: Condens. Matter **80**, 373 (1990).

[28] R. Proksch, E. Runge, P.K. Hansma, and S. Foss, J. Appl. Phys. **78**, 3303 (1995).

[29] M. Kleiber, F. Kummerlen, M. Lohndorf, A. Wadas, D. Weiss, and R. Wiesendanger, Phys. Rev. B **58**, 5563 (1998).

[30] C.A. Ross, M. Farhoud, M. Hwang, Henry I. Smith, M. Redjdal, and F.B. Humphrey, J. Appl. Phys. **89**, 1310 (2001).

[31] Jing Shi, S. Tehrani, and M.R. Scheinfein, Appl. Phys. Lett. **76**, 2588 (2000).

[32] J.A. Johnson, M. Grimsditch, V. Metlushko *et al.*, Appl. Phys. Lett. **77**, 4410 (2000).

[33] K.J. Kirk, J.N. Chapman, S. McVitie, P.R. Aitchison, and C.D.W. Wilkinson, Appl. Phys. Lett. **75**, 3683 (1999); K.J. Kirk, J.N. Chapman, and C.D. Wilkinson, *ibid.* **71**, 539 (1997).

[34] We assign ± 1 to the single domain state and 0 to the low moment state. The results are usually averaged over 500 individual particles.

[35] J. Shi, J. Li, and S. Tehrani, J. Appl. Phys. **91**, 7458 (2002).

[36] E.C. Stoner and E.P. Wohlfarth, Philos. Trans. R. Soc. London, Ser. A **240**, 599 (1948).

[37] http://math.nist.gov/oommf. We used the three dimensional code OXSII 1.2.

[38] N.A. Usov, C. Chang, and Z. Wei, J. Appl. Phys. **89**, 7591 (2001).